Sate-Space Modelling and Design of a 10MHz 180W Class E DC/DC Converter using WBG Devices

Samer Aldhaher and Paul D. Mitcheson

***Abstract*—This paper describes the modelling and design of a load-independent Class E DC/DC converter. Load-independent Class E circuits are able to maintain zero-voltage switching (ZVS) for any load value without requiring tuning or use of a feedback loop, and simultaneously achieve a constant amplitude AC voltage. This gives the ability for converters to maintain efficient operation and have inherently regulated outputs under varying load conditions. When used with wide-bandgap (WBG) devices, such as GaN and SiC, load-independent Class E circuits can operate efficiently at tens of megahertz (MHz) thus high power density 'credit card' sized converters can now be realised. Here we will present a 180 W capable load-independent Class E boost converter switching at 10 MHz and implemented entirely on a aluminium-core PCB with GaN and SiC devices.**

I. Introduction

The availability of WBG devices such as GaN and SiC is accelerating the trend towards increasing the switching frequency from the hundreds of kHz region to the tens of MHz region to obtain higher power densities and improved form factors. However traditional switch-mode topologies present a challenge towards operating at MHz frequencies since they become inefficient due to increased switching loss and switch-node ringing, and their performance significantly degrades due to circuit parasitics. Resonant conversion topologies based on Class E and Class EF are suited for operation at higher frequencies as they consist of a single low-side switch which is easy to drive, do not suffer from switch ringing at turn-off, can absorb circuit parasitics, operate at ZVS and can be designed to draw a low ripple DC current from the voltage supply. Furthermore, drive timings are relaxed therefore the gate driver and signal generation circuitry complexity is significantly reduced compared to traditional hard switching topologies. A complete Class E or Class EF circuit can be fabricated on a single layer printed circuit board (PCB) allowing full metal core PCBs to be used for improved thermal performance.

Class E and EF circuits are known to operate efficiently at MHz frequencies however at a single or narrow load range. The efficiency drops significantly for large variations in the load as the optimum switching conditions are lost. In fact it can be seen from recent work in the literature [1]–[7] that DC/DC converters built using Class E circuits operate at power levels below $30\,\mathrm{W}$ due to increased power loss as the load varies significantly, they also implement control methods such as on-off control to achieve voltage regulation. Consequently they do not achieve high power densities even when used with WBG devices.

It was shown in [8], [9] that the Class E and Class EF_2 circuits can operate at a wider load range delivering a constant amplitude AC voltage across the load while maintaining ZVS. This operation mode is referred to as 'load-independent' operation and is achieved by using a finite-DC choke and relaxing the requirement for zero-derivative voltage switching (ZDS) to ZVS only. Further work was carried out in [10] showing that Class EF circuits can also be designed to be load-independent and can deliver a constant amplitude sinusoidal current at reduced stresses. Having a constant current output is beneficial in applications such as WPT where a large alternating current is required to drive the transmitting coil.

The analysis of Class E and Class EF circuits is widely covered in the literature [11], [12] using analytical methods. The state-space modelling approach has been used recently in several publications in analysing Class E inverters and DC/DC converters [13], [14], it is capable of providing accurate results for any loaded Q values, different duty cycles and for any loading condition. In this paper will we will present a state-space model of the load-independent Class E converter operating at low loaded Q values (below 2) to derive component values that achieve load-independent operation. A design example will then be presented for a $180\,\mathrm{W}$ Class E DC/DC converter that can provide a DC output voltage with a good degree of inherent regulation without implementing a feedback loop. The converter will operate at $10\,\mathrm{MHz}$ and convert a input DC voltage of $40\,\mathrm{V}$ to $110\,\mathrm{V}$.

II. State-Space Modelling

Fig. 1a shows the circuit diagram of the load-independent Class E DC/DC converter. The circuit consists of a Class E inverter with finite-choke and a Class D voltage-driven rectifier. The inverter generates a AC output voltage which the rectifier then converts to a DC voltage. If the output voltage of the inverter is constant and does vary with load, then the rectified voltage will be fixed and independent of the load.

Fig. 1b shows the equivalent circuit of the converter for state-space modelling. The rectifier has been replaced by a resistor R_L which represents its input resistance. R_L is equal to 0.2026 times the DC load resistance as shown in [15]. Capacitor C_3 represents the total junction capacitance of the diodes and resistors r_{L_1} and r_{L_2} represent the loss in inductors L_1 and L_2 respectively.

978-1-5386-1180-7/18/$31.00 ©2018 IEEE

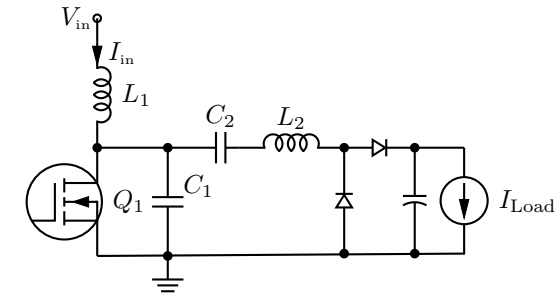

(a) circuit

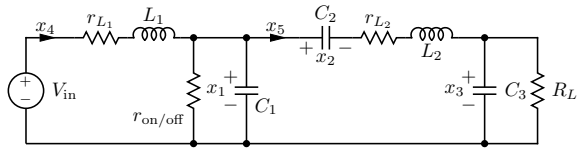

(b) equivalent circuit for state-space modelling including loss in inductors and parasitic capacitance of the diodes

Fig. 1. The load-independent Class E DC/DC converter. The converter consists of a load-independent Class E inverter and a Class D rectifier

The circuit has a set of state-space equations for each switching period. The general state-space representation for the on and off periods is

$$\dot{\mathbf{x}}_{\text{on/off}}(\omega t) = A_{\text{on/off}}\mathbf{x}(\omega t) + B_{\text{on/off}}\mathbf{u}(\omega t) \quad (1)$$

$$\mathbf{y}_{\text{on/off}}(\omega t) = C_{\text{on/off}}\mathbf{x}(\omega t) + D_{\text{on/off}}\mathbf{u}(\omega t) \quad (2)$$

where $\mathbf{x}$ is the state vector and contains the following six voltage and current state variables

$$\mathbf{x}(\omega t) = \begin{bmatrix} x_1(\omega t) & x_2(\omega t) & x_3(\omega t) & x_4(\omega t) & x_5(\omega t) \end{bmatrix}^T = \begin{bmatrix} V_{DS}(\omega t) & V_{C_2}(\omega t) & V_{C_3}(\omega t) & I_{L_1}(\omega t) & I_{L_2}(\omega t) \end{bmatrix}^T \quad (3)$$

and matrices A, B, C and D are equal to

$$A_{\text{on/off}} = \begin{bmatrix} \frac{1}{\omega C_1 r_{\text{on/off}}} & 0 & 0 & \frac{1}{\omega C_1} & -\frac{1}{\omega C_1} \\ 0 & 0 & 0 & 0 & \frac{1}{\omega C_2} \\ 0 & 0 & -\frac{1}{\omega C_3 R_L} & 0 & \frac{1}{\omega C_3} \\ -\frac{1}{\omega L_1} & 0 & 0 & -\frac{r_{L_1}}{\omega L_1} & 0 \\ \frac{1}{\omega L_2} & -\frac{1}{\omega L_2} & -\frac{1}{\omega L_2} & 0 & -\frac{r_{L_2}}{\omega L_2} \end{bmatrix} \quad (4)$$

$$B_{\text{on}} = B_{\text{off}} = \begin{bmatrix} 0 & 0 & 0 & \frac{V}{\omega L_1} & 0 \end{bmatrix}^T \quad (5)$$

$$C_{\text{on}} = C_{\text{off}} = \mathbf{I}, \qquad D_{\text{on}} = D_{\text{off}} = 0 \quad (6)$$

The general solution to 1 and 2 is given by

$$\mathbf{x}(\omega t) = \mathbf{x_n}(\omega t) = e^{A\omega t}\mathbf{x}(0) + A^{-1}\left(e^{A\omega t} - \mathbf{I}\right)B. \quad (7)$$

The initial condition matrix $x(0)$ can be determined by applying the continuity conditions of the voltages and current of the capacitors and inductors as shown in [14]. For load-independent operation; constant ZVS, the initial conditions of the following states for the on and off periods should equal zero to over the entire load range

$$x_{1_{\text{on}}}(0) = x_{1_{\text{off}}}(0) = 0 \quad \text{for } R_L = \{R_{\min}, \infty\} \quad (8)$$

where $R_{\min}$ is the minimum load resistance at which the converter delivers the maximum power. By solving the initial conditions for the above criteria, the values of the components can be calculated. Fig. 2 shows switch voltage and current waveforms and the output AC voltage of the load-independent Class E inverter operating at a low loaded Q factor. The duty cycle is $50\,\%$ and the input voltage is $40\,\text{V}$. It can be seen that the inverter maintains ZVS for different loading conditions from open circuit load condition to the minimum load resistance. The amplitude of the output AC voltage also remains fairly constant and is not sinusoidal.

III. Design of a Constant DC voltage 10 MHz 180W Class E DC/DC Converter

Having performed the state-space modelling and analysis, here we will present the design of a Class E converter that is capable of converting a input voltage of $40\,\text{V}$ to $110\,\text{V}$ switching at $10\,\text{MHz}$. The converter will provide up $180\,\text{W}$ of power and will be implemented entirely on an aluminium-core PCB for improved thermal performance. The dimensions of the PCB are $50\,\text{mm}$ X $35\,\text{mm}$ X $1.5\,\text{mm}$.

At $110\,\text{V}$ output DC voltage the DC load resistance that will consume $180\,\text{W}$ is $67.2\,\Omega$. Consequently the input resistance

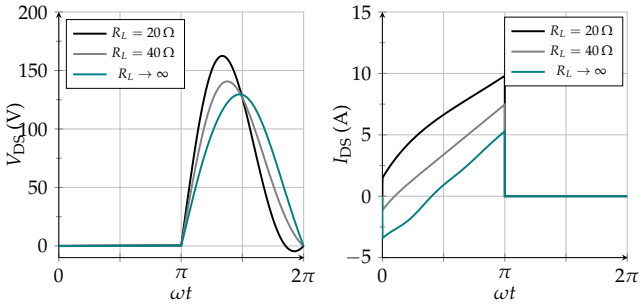

(a) switch voltage and current

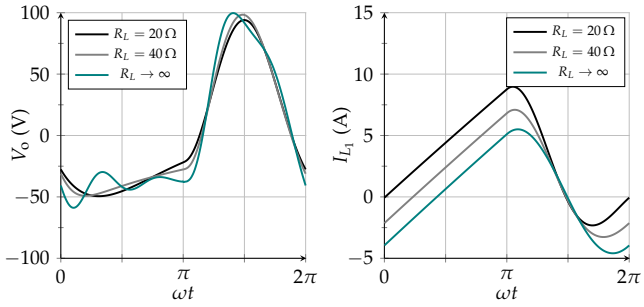

(b) output voltage and inductor L_1 current

Fig. 2. Voltage and current waveforms of the load-independent Class E inverter operating at low loaded Q factors (below 2) at different loading conditions

of the rectifier which will be the minimum AC load resistance seen by the inverter is 13.6 Ω. Diodes with low forward voltage and more importantly lower junction capacitance need to be used here. The C3D1P7060Q (600 V/1.7 A) SiC diodes from Wolfspeed are selected, two diodes are connected in parallel for each branch of the Class D rectifier to limit the temperature rise. The diode's junction capacitance according to the datasheet is 10 pF at 110 V, thus the total capacitance of four diodes is 40 pF. Assuming a parasitic capacitance of 10 pF the value of capacitor C_3 is now 50 pF.

Magnetic core inductor are suitable for switching frequencies in the kHz region to the lower MHz region. At 10 MHz air-core inductors should be used. We find the 2014VS series of air-core power inductors from Coilcraft to be suitable. We choose the highest value available which is 257 nH for inductors L_1 and L_2. Using lower inductor values will lead to higher current stresses and higher conduction losses which can reduce the efficiency. The equivalent series resistance of both inductors at 10 MHz is approximately 0.160 Ω.

The values of C_1 and C_2 that will result in load-independent operation can now be calculated from the state-space model and are given in Table I. Inductor L_2 was increased to 270 nH in the model to account for parasitic inductance in the PCB. The loaded Q factor at minimum load resistance, or at maximum power is 1.19.

The switch used is the GS66508B(650 V/30 A) GaNfet from GaN Systems with the UCC27512 gate driver from Texas Instruments. Fig. 3 shows a photograph of the implemented Class E DC/DC converter. The converter was implemented entirely on a 1.5 mm thick aluminium-core PCB, no heatsink is required.

IV. Experimental Results

Table I lists the implemented component values. The implemented values of C_1 and C_2 are lower than their designed values due to the GaN fet's output capacitance and the higher parasitic capacitance of the aluminium core PCB. The BK Precision 8512 electronic load was used to evaluate the converter and the switching signal was supplied from a function generator. The gate voltage was 6 V. It was found

TABLE I
Calculated and Implemented Component Values

Component	Calculated	Implemented	Description
C_1 (pF)	651	480	Vishay QUAD HIFREQ Series
C_2 (nF)	1.76	1.6	Vishay QUAD HIFREQ Series
C_3 (pF)	50	-	Diode + parasitic capacitances
L_1 (nH)	257	257	Coilcraft 2014VS Series
L_2 (nH)	270	257	Coilcraft 2014VS Series
f (MHz)	10	10	
V_{in} (V)	40	40	
Q_1	GS66508B (650 V, 30 A)		GaN Systems
Diodes	C3D1P7060Q (60 V, 1.7 A)		Wolfspeed

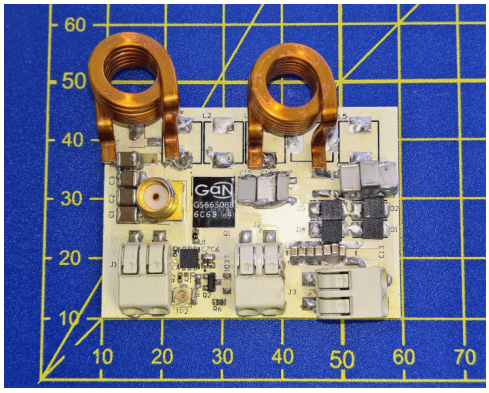

Fig. 3. Photograph of the implemented Class E DC/DC converter. The dimensions of the aluminium-core PCB are 50 mm X 35 mm X 1.5 mm.

that the electronic load could not maintain a stable load current at values below 0.8 A, this is thought to be due to the high frequency ripple in the output voltage of the converter and due to the low control bandwidth of the electronic load which led to oscillations in the output voltage.

Fig. 4 shows the measured switch drain waveform over the load range 0.8-1.5 A, it can be seen that ZVS is maintained and load-independent operation is achieved.

Figs. 5 and 6 show the measured output voltage, power and efficiency over the load current range from 0.8-1.5 A. All measurements were obtained without any adjustments to the switching frequency, duty cycle and to the components. The output DC voltage is approximately 130 V at 0.8 A load current and decreases to approximately 110 V at 1.55 A. The efficiency remains fairly constant at approximately 90 % over the load range.

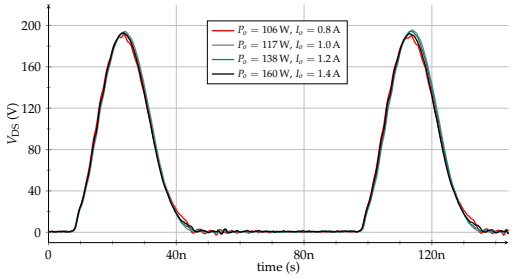

Fig. 4. Experimental waveforms of the Class E DC/DC converter

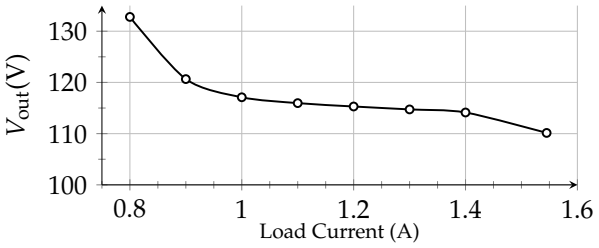

Fig. 5. Measured output voltage

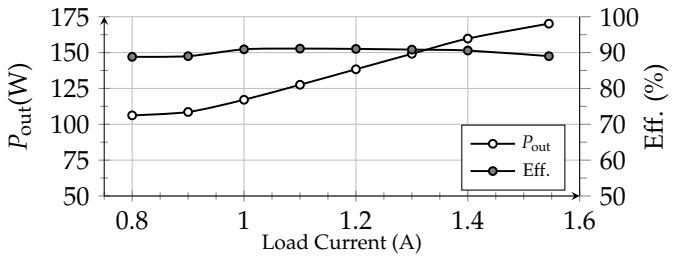

Fig. 6. Measured output power and efficiency

Fig. 7 shows a steady-state thermal image at 170 W load power. The input power was 191 W. The components with highest temperate are the SiC diodes at 96 °C, the estimated power loss in the diodes are 10 W. The rest of the losses are in inductors L_1 and L_2.

The Class E DC/DC converter was not implemented with a feedback control loop. Improved output regulation can be achieved using on-off control which has been the common control method applied in recent MHz converters [1]–[5] however at the expense of increased circuit complexity.

V. Conclusions & Future Work

Class E circuits are known to operate efficiently at MHz frequencies however over a narrow load range only, ZVS is lost and efficiency degrades as the load varies from its optimum value. The concept of load-independent operation for Class E circuits allows for operation over a much wider load range by the relaxing the optimum switching condition to ZVS only. This allows for MHz DC/DC converters to be implemented using WBG devices to achieve higher power densities with good output regulation features without tuning or adjustment of values. A state-space model of a load-independent Class E DC/DC converter has been presented which takes into account the loss in components and parasitic capacitances. The state-space model provides higher accuracies when calculating component values and determining losses especially when operating at low loaded Q factors. The design of a 180 W Class E DC/DC converter switching at 10 MHz has been presented to show the advantage of using the load-independent Class E circuits with GaN and SiC devices. The converter was implemented entirely on aluminium-core pcb with dimensions smaller than a 'credit card'. Future work may include using PCB inductors to achieve a improved form factor and improving the performance of converter.

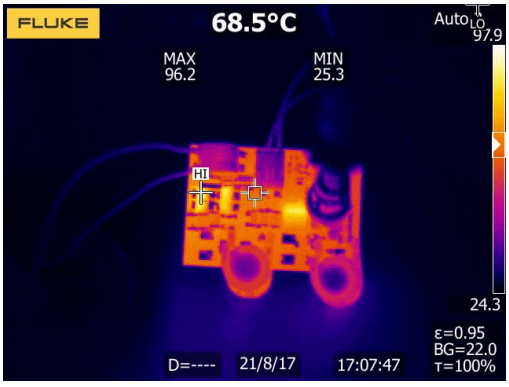

Fig. 7. Thermal steady-state image of the converter at 180 W. The SiC diodes have the highest temperature at 96 °C

Acknowledgement

This research was funded by EPSRC Converter Architectures grant ref. EP/R004137/1 and EPSRC Underpinning Power Electronics 2012: Components Theme Power grant ref. EP/K034804/1.

References

[1] K. H. Lee and J. I. Ha, "Analysis and design of resonant rectifier for high-frequency DC/DC converters," in *IEEE App. Power Electron. Conf. Expo. (APEC)*, Mar. 2017, pp. 2475–2480.

[2] Y. Guan, Y. Wang, W. Wang, and D. Xu, "Analysis and design of high frequency DC/DC converter based on resonant rectifier," *IEEE Trans. Ind. Electron.*, pp. 1–1, to be published 2017.

[3] Z. Zhang, X. W. Zou, Z. Dong, Y. Zhou, and X. Ren, "A 10 MHz eGaN isolated Class ϕ_2 dcx," *IEEE Trans. Power Electron.*, vol. 32, no. 3, pp. 2029–2040, Mar. 2017.

[4] Z. Zhang, J. Lin, Y. Zhou, and X. Ren, "Analysis and decoupling design of a 30 MHz resonant SEPIC converter," *IEEE Trans. Power Electron.*, vol. 31, no. 6, pp. 4536–4548, Jun. 2016.

[5] J. Zhao and Y. Han, "A novel switched-capacitor based partial power architecture for a 20 MHz resonant SEPIC," in *IEEE Energy Conv. Con. Expo. (ECCE)*, Sep. 2015, pp. 1442–1449.

[6] A. Knott, T. M. Andersen, P. Kamby, J. A. Pedersen, M. P. Madsen, M. Kovacevic, and M. A. E. Andersen, "Evolution of very high frequency power supplies," *IEEE Trans. Emerg. Sel. Topics Power Electron*, vol. 2, no. 3, pp. 386–394, Sep. 2014.

[7] Z. Zhang, K. D. T. Ngo, and J. L. Nilles, "A 30 W flyback converter operating at 5 MHz," in *IEEE Appl. Power Electron. Conf. Expo.*, Mar. 2014, pp. 1415–1421.

[8] R. E. Zulinski and K. J. Grady, "Load-independent Class E power inverters: Part I. Theoretical development," *IEEE Trans. Circuits Syst. I, Reg. Papers*, vol. 37, no. 8, pp. 1010–1018, Aug. 1990.

[9] L. Roslaniec, A. S. Jurkov, A. Al Bastami, and D. J. Perreault, "Design of single-switch inverters for variable resistance/load modulation operation," *IEEE Trans. Power Electron.*, vol. 30, no. 6, pp. 3200–3214, Jun. 2015.

[10] S. Aldhaher, G. Kkelis, D. C. Yates, and P. D. Mitcheson, "Class EF_2 inverters for wireless power transfer applications," in *IEEE Wireless Power Transfer Conference (WPTC)*, May 2015, pp. 1–4.

[11] M. K. Kazimierczuk, *RF Power Amplifiers*, 2nd ed. Chichester, UK: John Wiley & Sons Ltd, 2015.

[12] A. Grebennikov, N. O. Sokal, and M. J. Franco, *Switchmode RF and Microwave Power Amplifiers*. Oxford, UK: Academic Press, 2012.

[13] P. Reynaert, K. L. R. Mertens, and M. S. J. Steyaert, "A state-space behavioral model for cmos class e power amplifiers," *IEEE Trans. Comput. Aided Design Integr. Circuits*, vol. 22, no. 2, pp. 132–138, Feb. 2003.

[14] P. C. K. Luk, S. Aldhaher, W. Fei, and J. F. Whidborne, "State-space modeling of a class bfE^{bf2} converter for inductive links," *IEEE Trans. Power Electron.*, vol. 30, no. 6, pp. 3242–3251, Jun. 2015.

[15] M. K. Kazimierczuk and D. Czarkowski, *Resonant Power Converters*. Wiley, 2011.